/ws5/ms/triton50 Edition of June 24, 1995

Chapter for Ices In the Solar System volume NASA-TM-112309

THE SURFACE COMPOSITIONS OF TRITON, PLUTO, AND CHARON

Dale P. Cruikshank
NASA Ames Research Center, MS 245-6
Moffett Field, CA 94035-1000, USA
e-mail: cruikshank@ssa1.arc.nasa.gov
Phone: 415-604-4244, FAX 415-604-6779

Ted L. Roush
San Francisco State Univ. and NASA Ames Research Center
Moffett Field, CA 94035-1000, USA

Tobias C. Owen
Institute for Astronomy, University of Hawaii
2680 Woodlawn Dr.
Honolulu, HI 96822, USA

Eric Quirico
Laboratoire de Glaciologie et Géophysique de l'Environnement
54, rue Molière, Domaine Universitaire, B.P. 96
38402 Saint-Martin-d'Hères, France

Catherine DeBergh
Observatoire de Paris
5 Place Jules Janssen
92195 Meudon, France

ABSTRACT

Neptune's satellite Triton, and the planet-satellite binary Pluto and Charon, are the most distant planetary bodies on which ices have been directly detected. Triton and Pluto have very similar dimensions and mean densities, suggesting a similar or common origin. Through earth-based spectroscopic observations in the near-infrared, solid N_2, CH_4, and CO have been found on both bodies, with the additional molecule CO_2 on Triton. N_2 dominates both surfaces, although the coverage is not spatially uniform. On Triton, the CH_4 and CO are mostly or entirely frozen in the N_2

matrix, while CO_2 may be spatially segregated. On Pluto, some CH_4 and the CO are frozen in the N_2 matrix, but there is evidence for additional CH_4 in a pure state, perhaps lying as a lag deposit on a subsurface layer of N_2. Despite their compositional and dimensional similarities, Pluto and Triton are quite different from one another in detail. Additional hydrocarbons and other volatile ices have been sought spectroscopically but have not yet been detected. The only molecule identified on Pluto's satellite Charon is solid H_2O, but the spectroscopic data are of low precision and admit the presence of other ices such as CH_4.

1. Introduction

Contemporary models of the chemistry of the Solar System incorporate the concept of the "ice line", that is, the distance from the Sun beyond which water ice is stable against evaporation for the age of the planets, approximately 4.6 Gyr. The ice line concept arose not entirely from theoretical considerations, but also from a growing body of observational results demonstrating the inactivity of icy comets at great distances from the Sun, large expanses of solid H_2O on the surfaces of some of the Galilean satellites, and the apparent absence of ice on the asteroids. Thus, the ice line occurs at about 5 AU from the Sun; Jupiter's mean heliocentric distance is 5.20 and the minimum is 4.95 AU.

The stability of an ice in the Solar System depends not only on the distance from the Sun, but even more importantly upon the volatility of the ice. At a temperature of 60 K the vapor pressures of simple pure ices (N_2 to H_2O) range over 30 orders of magnitude, while at T = 40 K the range increases to 50 orders of magnitude. Thus, the concept of an ice line is simplistic and serves primarily to alert us to the likelihood that volatile simple molecules composed of the cosmically abundant elements are major constituents of the bodies of the colder regions in the Solar System beyond about 5 AU. A large body of spacecraft investigations, Earth-based telescopic studies, and theoretical considerations continue to establish and strengthen this supposition.

In this paper we review the current understanding of three large icy bodies at the outer margin of the system of major planets, Neptune's satellite Triton, and the binary planetary system of

Pluto and Charon. The section on Triton draws upon the recent review by Brown et al. (1995), while the discussion of Pluto and Charon incorporates material from the review by Cruikshank et al. (1996).

Triton was studied by the Voyager 2 spacecraft in 1989, yielding information of direct relevance to Pluto, which has not yet been the target of a spacecraft investigation. Direct identification of the ices on all three of these bodies has come from Earth-based telescopic observations through near-infrared spectroscopy, while the role of ices in the bulk compositions is being developed through a wide variety of observational and theoretical approaches. The interaction of the condensed volatiles on the surfaces of Triton and Pluto with their atmospheres is not a central consideration of this paper, though such studies are clearly an important part of the larger picture of the behavior of volatiles on planetary surfaces.

2. Triton

Triton is the largest satellite of Neptune, with a diameter of 2705 km (Stone and Miner 1989, McKinnon et al. 1995). It moves in a circular (retrograde) orbit that is inclined 157 degrees to Neptune's equator. The orbital period of 5.877 days is the same as Triton's period of rotation, so that the satellite keeps one hemisphere directed toward Neptune at all times. Prior to the Voyager 2 encounter with Neptune and Triton in 1989, little was known about the composition, temperature, or even the dimensions of Triton. Spectroscopy from Earth had shown condensed nitrogen and methane on its surface (Cruikshank et al. 1984), from which the presence of these two molecules in a tenuous atmosphere was deduced, but nothing was known of the atmospheric density or structure.

Voyager revealed Triton as a frozen world with a geologically fresh surface nearly devoid of impact craters, and showing evidence of episodes of local and possibly global melting (Stone and Miner 1989, Smith et al. 1989). The tenuous N_2 and CH_4 atmosphere has a photochemical haze layer, discrete clouds, and seasonal sublimation-driven winds that waft the effluent from at least three active plumes from the south polar region toward the equator. Overall, the atmosphere is sufficiently transparent to permit a clear view of the surface. Voyager yielded an atmospheric surface pressure of about 14 microbar of N_2

(Broadfoot et al. 1989) which is in approximate vapor pressure equilibrium with the N_2 ice on the surface. Voyager carried no instruments that detected surface ices directly; information on the composition of the surface constituents comes entirely from specroscopy from Earth-based or Earth-orbital facilities.

Infrared spectroscopy in the region 0.8-3.5 μm, which probes the uppermost several millimeters of the surface from which incident sunlight is scattered, shows the presence of four different condensed molecules in the form of ice. Solid CH_4 was the first ice found (Cruikshank and Silvaggio 1979, Cruikshank and Apt 1984), because of its intense spectral absorption bands, and later N_2 was identified through the presence of the 2.16 μm band, also seen in absorption (Cruikshank et al. 1984). Cruikshank et al. (1984) found that a model of Triton's spectral continuum required addition of a component of H_2O ice in the form of a fine-grained frost. Spencer et al. (1990) found additional evidence for solid CH_4 in the 3-μm region. Following the Voyager flyby, major improvements in astronomical spectroscopic instruments yielded the discovery of absorption bands of CO and CO_2 in Triton's spectrum (Cruikshank et al. 1993), as shown in Figure 1. In addition, Stern (1993) has suggested that Triton's low albedo in the ultraviolet (lam < 0.3 μm) may indicate the presence of condensed SO2, but a unique spectroscopic identification has not yet been made.

Quantitative analysis of multi-component ices can be accomplished by computatiion of synthetic spectra of scattering surfaces using the real and imaginary indicies of refraction of the known components (measured in the laboratory) and a scattering theory such as that developed by Hapke (1993a,b). We defer a detailed discussion of the techniques used in the model work discussed in here to the Appendix, but the main results are presented here.

The first rigorous scattering models of Triton's near-infrared spectrum were presented by Cruikshank et al. (1993). Three types of models were calculated; (1) "checker-board" models consisting of spatially segregated patches of the four clearly identified ices (not including H_2O), such that a single photon is scattered from a grain of only one species of ice; (2) "salt and pepper" models of scattering from intimate mixtures in which a photon scattered from one kind of grain may also be scattered from grains of different composition; and (3) models of ices in which a single grain contains more than one kind of molecule.

While the initial models presented by Cruikshank et al. (1993) are not uniquely constrained, variations in input parameters, such as grain size, mass fractions of the four components (not including H_2O), fractions of the surface covered by individual components, etc. were explored. While the behaviors of the absorption bands of the various components are closely interrelated, it is convenient to consider each of the four identified molecules individually before converging on a single model that best describes the observed spectrum.

2.1 Nitrogen

Molecular nitrogen is the most volatile constituent identified in the spectrum. Condensation and sublimation of the N_2 appear to maintain an approximately isothermal surface, even on the night hemisphere and in the currently dark north polar zone (Trafton 1984). The N_2 band observed on Triton has a central wavelength of 2.1477 μm, which is identical within the experimental errors to the laboratory wavelength of 2.1478 μm for the beta phase of N_2 (Green et al. 1991; Tryka et al. 1993; Grundy et al. 1993a,b).

At low pressure, solid N_2 exists in two distinct phases; below the transition temperature of 35.6 K the cubic alpha phase exists, and above that temperature the less dense hexagonal beta phase occurs. The spectrum of alpha N_2 is characterized by a very narrow absorption superimposed upon an broad, weaker absorption band that has a characteristic temperature-dependent profile (Grundy et al. 1993a,b; Löwen et al. 1990) The absorption band in beta N_2 is much broader and also sensitive to temperature (Tryka et al. 1993, 1994; Grundy et al. 1993a,b). At temperatures near the triple point (63.15 K), the absorption is weak, broad and centered at 2.151 μm; at lower temperatures the band becomes narrower and shifts to a central wavelength of 2.148 μm. Between about 40K and 36 K, a weak component of the band appears at 2.162 μm on the long wavelength wing of the main band. Tryka et al.(1994) showed that beta N_2 at 38 K gave the best fit to the Triton spectrum.

The question of the assignment of the absorption bands in the 2.15 μm region to α and β phases of solid N_2 was recently reviewed and discussed by Quirico et al. (1995). For the α phase, the authors proposed a tentative identification for the obgserved absorption bands, but this was not possible for the β

phase because the physics of this disordered phase is still poorly known. It was also pointed out that the infrared activity of the strong and narrow 2.148 μm band could be induced by crystal defects. Therefore, if high quality crystals of α N_2 exist on Triton, the band would either not appear at all, or would appear at strongly reduced intensity. For the β phase, they showed that the broad absorption band around 2.15 μm is intrinsic to solid N_2 near the melting point (63.15 K), but this was not demonstrated near the β-α phase transition. Considering these differing views, it appears that the issues of the phase of N_2 ice and of its temperature are not yet completely solved.

We note here that there is presently no direct evidence for the occurence of α N_2 on Triton, but Quirico and Schmitt (1995) showed that the frequency of the CH_4 bands better fit CH_4 diluted in α N_2. Indeed, both phases may occur simultaneously on the surface if vertical, and/or horizonal regions exist at temperatures above and below the phase-transition temperature, which is very close to the measured temperature of the surface (Duxbury and Brown 1993). Again we note that the N_2 phase and temperature are not yet entirely resolved.

The model calculations show that N_2 ice dominates the surface layer. The reflectance at the bottom of the N_2 band in Triton's spectrum is about 85% of the nearby continuum. Using this depth of absorption with the known absorption coefficient at the center of the N_2 band (0.02 cm-1) we find that a photon of 2.148 μm wavelength entering Triton's surface traverses an average of about 15 cm of solid N_2 before emerging from the surface. The N_2 particle size derived from the scattering model calculations is of order 1 cm, if isotropic scattering dominates radiative transport within the nitrogen.

2.2 Methane

Numerous bands attributed to solid CH_4 are seen in Triton's spectrum. Gaseous CH_4 is a trace component of the atmosphere (Broadfoot et al. 1989) and models derived from Voyager UVS data (Herbert and Sandel 1991) suggest that at the surface methane is close to saturation or slightly undersaturated relative to the vapor pressure of gas over pure CH_4 ice. Undersaturation would suggest that methane is not exposed as a free ice, but is instead complexed in some way with another constituent. The possibility that CH_4 is complexed with N_2 arose independently from the

observation that the methane bands in Triton's spectrum are systematically shifted to shorter wavelengths than found in the laboratory for pure CH_4 (Cruikshank et al. 1993). (Note that in the 1993 paper by Cruikshank et al. the shift is incorrectly stated as toward longer wavelengths.) Laboratory spectra of very dilute mixtures of CH_4 (0.25% and less) in N_2 show this matrix shift by a similar amount, which is different from one band to another (Schmitt and Quirico 1992). Methane is highly soluble in N_2, and the natural occurrence of solid solutions of these two is expected on Triton, where cycles of sublimation and condensation occur.

A systematic study of the near-infrared spectra of CH_4 diluted in N_2 as a function of temperature (15-63K), crystalline phase and formation process was recently performed by Quirico and Schmitt (1995). Their results show that the peak frequencies of all the CH_4 bands are significantly shifted with respect to pure solid CH_4, but also that the peak frequency, the width, the intensity and the band countour of each band were found to depend on these physical parameters. For example, the band around 2.315 μm is highly sensitive to the crystalline phase of the N_2 matrix (a jump of about 0.045 μm occurs at the β-α transition at 35.6 K), whereas the band around 2.372 μm is virtually unaffected. In addition, the peak of the nu_3+v_4 band was found to be strongly temperature dependent in α N_2 (near the α-β transition), and almost independent of temperature in β N_2. A very different behavior is found for the 1.690 μm band of pure CH_4, which completely disappears for CH_4 isolated in the N_2 matrix.

The comparison between the peak frequencies of the CH_4 bands of Triton's spectra with those measured in laboratory spectra confirms that, on Triton, CH_4 is diluted in N_2 at very low concentration, and further prove the absence of significant of pure CH_4 ice at the surface. On the other hand, this spectroscopic analysis would sugdgest that most of the CH_4 is diluted in α N_2 close to, or at, the α-β transition temperature (Quirico and Schmitt 1995), in contradiction to the phase (β N_2) and the temperature of Triton's ices (~38 K) derived from the nitrogen band itself (Grundy et al. 1993a,b; Tryka et al. 1993, 1994).

Cruikshank et al. (1993) used optical constants for CH_4 that were artifically adjusted to account for the matrix shift of the central wavelengths of the several bands, because optical

constants for true molecular mixes of CH_4 in N_2 were not available. They could not achieve a fully satisfactory match of all the CH_4 band strengths with the Triton spectrum for a single choice of CH_4 abundance and effective grain size. The intimate mixture model that best fit the original Triton data had an abundance of 0.05% CH_4 relative to N_2, with an uncertainty of a factor of 2 to 4. Detailed modeling of the spectra, using optical constants of N_2:CH_4:CO solid solutions are underway (Doute et al., in preparation).

The very low abundance of CH_4 derived on the basis of band strengths is consistent with the matrix wavelength shift of the CH_4 bands when dissolved in N_2. Further, the absence of broadening or doubling of the CH_4 bands on Triton indicates that most, but perhaps not all of the methane is incorporated in the matrix.

2.3 Carbon Monoxide

The (2-0) band of CO at 2.35 μm is clearly seen in Triton's spectrum, and the (3-0) band shows weakly in a blend with a band of CO_2 (see below). Laboratory spectra of CO diluted in a N_2 matrix (1% CO), recorded between 25 and 63 K, show that the bands are only slightly shifted with respect to pure solid CO (less than 2.5 cm^{-1}) but that the band FWHM strongly depend on phase and temperature (Quirico and Schmitt 1995). The N_2 matrix shift of these CO band wavelengths is below the spectral resolution of the existing Triton data. Therefore the spectra cannot distinguish between free CO on the surface or CO in the N_2 matrix. The relative fraction of CO to N_2 in the best intimate mixture model by Cruikshank et al. (1993) is 0.1%, with an uncertainty of a factor of 2 to 4.

Broadfoot et al. (1989) derived an atmospheric mixing ratio of CO to N_2 of <0.01, while at 38 K the ratio of vapor pressures is 0.074 (Brown and Ziegler 1979). This disparity between the vapor presures and the atmospheric mixing ratios suggests that the condensed CO is complexed with another constituent, probably the N_2.

2.4

Four bands of CO_2 ice are found in Triton's spectrum; 1.577, 1.966, 2.012, and 2.070 μm (Cruikshank et al. 1993). If CO_2 is

included in the molecular mix scattering models as a fourth component, its derived relative fraction to N_2 is ~0.1%. However, because CO_2 is some 24 orders of magnitude less volatile than N_2 at the relevant temperature, this solid will not sublime and condense in the same way that the more volatile components are expected to do as Triton undergoes its seasonal and diurnal cycles. Thus, CO_2 is likely to occur on Triton's surface in exposures independent of the N_2 mixture. The best models by Cruikshank et al. (1993) therefore treat CO_2 (with grain size 0.8 mm) as a spatially isolated material covering approximately 10% of Triton's surface, with the N_2 mixture incorporating the CH_4 and CO covering the remaining 90%. Expanses of CO_2 ice may be exposed at the surface or seen through transparent overlayers of N_2.

2.5 Other Constituents

Photolytic products of CH_4 and N_2 in Triton's atmosphere might occur on the surface, where their further disintegration from ultraviolet sunlight could produce the geographical units of various colors identified in the Voyager images (Thompson and Sagan 1990). Cruikshank et al. (1993) found no evidence in Triton's specrum for various other ices, including C_2H_2, C_2H_4, C_2H_6, H_2O, H_2S, CH_3OH, and NH_3. As noted above, water ice was suspected in an earlier spectroscopic study by Cruikshank et al. (1984), but because of the limited continuum coverage in the data taken since 1991 it has not been recognized. Although H_2O is presumed to be a major constituent of Triton's interior, the question of its presence on the visible surface is not settled. If H_2O ice is present, it must appear as "bedrock", similar to solid CO, because its exceedingly low vapor pressure does not allow it to participate in the seasonal (or secular) sublimation and condensation processes in which the more volatile constituents engage.

Laboratory studies of possible minor amounts of various hydrocarbons in Triton's N_2 matrix were conducted by Schmitt and Quirico (1992), Bohn et al. (1994), and Quirico and Schmitt (1995). Bohn et al. compared differences between Triton's spectrum and the Cruikshank et al. (1993) models, particularly in the region near 2.3 μm. Although no specific molecules could be identified, Bohn et al. noted that a sequence of branched alkanes dissolved in N_2 matrix might account for the discrepancy between the models and the Triton spectrum. However, new models of the

Triton spectrum with the more relevant CH_4 data published by Quirico and Schmitt (1995) show that the unexplained absorptions in the wing and in the peak of the 4310 cm^{-1} (2.32 μm) CH_4 band is simply due to the shape of the band for CH_4 diluted in N_2 (Doute et al., in preparation). These preliminary studies provides a basis for further investigations as the quality of the telescopic data and the theoretical modelling increases. Another result of the Bohn et al. study was the recognition of a potentially important product of UV irradiation of N_2:CH_4 solid solutions in the ice phase. The energy-rich and highly reactive molecule diazomethane (CH_4N_2) may be responsible for synthesis of larger alkanes from CH_4, as well as driving chemical reactions in the surface toward hydrocarbon saturation. Diazomethane may be responsible for the removal of C_2H_4 and H_2CO expected to form in the aerosol suspended in Triton's atmosphere.

Although complex organic solids have not be firmly identified on Triton, the coloration of the surface and the character of the plume deposits is suggestive of their presence. Stable organics may be produced in the ices on the surface, or in the atmosphere. Specifically, the aerosol component of the atmosphere visible in Voyager images is probably the photochemical product of solar UV on gaseous CH_4 (Lunine et al. 1989; Sagan and Khare 1979; Sagan and Thompson 1984).

Two cosmically abundant volatiles that are undetectable in the wavelength regions studied are neon and argon. Neon has nearly the same cosmic abundance as nitrogen and has a much higher vapor pressure, but it does not dominate Triton's atmosphere. The fact that it does not is consistent with the difficulty in trapping neon in ice that forms at T > 25K. The ices that formed Triton, including any late cometary bombardment, were apparently formed at higher temperatures, as was the case for Pluto (Owen et al. 1993). Argon is 16 times less abundant than N_2, but could possibly be enriched on Triton if much of this body's N_2 has been lost to space. A search for an enrichment of $^{15}N/^{14}N$ would test the enrichment scenario, and experiments on the spectrum of Ar in N_2 could be conducted to see if there are any effects on the N_2 band at 2.148 μm.

2.6 Variability of Triton

Although the observational data base is quite small, there is clear evidence that the spectral reflectance (0.3-0.8 μm) of

Triton changed markedly sometime between 1979 and 1989 (Smith et al. 1989). Two contemporaneous but independent observations in 1979 are in good agreement that the spectral reflectance in the interval 0.3-0.8 μm increased markedly toward longer wavelengths, while color photometry from Voyager 2 and from a telescopic data set in 1989 are also in good mutual agreement but show a nearly neutral reflectance with very little slope. A more detailed discussion of the color variability is given by Brown et al. (1995).

Variability in Triton's near-infrared spectrum (0.8-2.5 μm) with the satellite's rotation was noted in the early (1980-1981), low-resolution spectra by Cruikshank and Apt (1984), but it is also possible that in the time interval represented by the data some major change occurred on Triton's surface. One possibility is that the condensation of CH_4-poor ice on a portion of Triton's surface in that time interval masked the methane bands, thus reducing their strength in the spectrum. This and other considerations are discussed in greater detail by Brown et al. (1995).

2.7 Triton--Summary

The high albedo and photometric properties (Brown et al. 1995) as well as the infrared spectrum of Triton all show that this satellite is entirely covered by a mixture of ices, of which N_2 is the dominant species. The ice is contaminated with coloring agents, possibly organic solids produced by photochemical reactions in the atmosphere and on the surface. The surface ices interact with the tenuous atmosphere of Triton on time scales probably related to the extreme seasonal cycles experienced by this body. Repeated cycling of Triton's volatiles from surface to atmosphere and back has produced an extraordinarily complex array of colored units and topographic structures that are geologically young. Impact craters are all but absent. Triton's bulk density is 2.06 g/cm^3 (McKinnon et al. 1995), indicating an internal composition that includes a large quantity of rocky material in addition to the volatiles (probably dominated by H_2O ice)

3. The Pluto-Charon Binary

Pluto and its satellite Charon constitute a binary planet system in which Pluto with a diameter of 1164 +/-22.9 km is almost

exactly twice the size of Charon at 621 +/-20.6 km (Young and Binzel 1994). Charon moves in a near-circular orbit about the common center of gravity of the pair. Pluto and Charon are in locked synchronous revolution and rotation, with both bodies keeping the same hemispheres directed toward one another throughout the rotation/revolution period of 6.390 days. The heliocentric orbit of this pair of objects carries them to a minimum distance of 29.67 AU and a maximum distance of 49.95 AU from the Sun.

Methane ice was discovered on Pluto in 1976 (Cruikshank et al. 1976) before the existence of the satellite was known, and before there were useful estimates of the mass or diameter. Two years later, Christy and Harrington (1978) discovered Charon, permitting a calculation of the mass of Pluto and setting the stage for the epoch of mutual transits and eclipses in the mid-1980s. From those mutual events, many important facts about the pair of bodies was established, not the least of which was their dimensions. The resulting bulk density of Pluto is 2.0 g/cm3, or nearly the same as Triton. The diameter of Pluto is also nearly the same as Triton.

3.1 Pluto

Near-infrared (0.8-2.5 μm) spectra of Pluto in the 1980s demonstrated the presence of solid CH_4, showing bands that are significantly stronger than the corresponding bands on Triton (Cruikshank and Silvaggio 1980, Soifer et al. 1980). Buie (1984) found that the 0.619 and 0.725 μm CH_4 bands vary in strength as the planet rotates, establishing that they arise from surface ice rather than from the atmosphere. The methane bands between 0.8 and 2.5 μm also vary in synchronism with Pluto's rotational lightcurve (measured at visible wavelengths), showing that the CH_4 abundance is at least approximately correlated with the highly reflective areas of the planet (Buie and Fink 1987, Marcialis and Lebofsky 1991, Cruikshank and Brown [unpublished]).

For several years CH_4 was thought to be the principal surface constituent, but when the refractivity of the atmosphere was measured by a stellar occultation in 1988 (Elliot et al. 1989) it became clear that the major component is something else. Nitrogen was suspected, but not until a major advance in spectroscopic instrumentation was applied to Pluto were hidden details of the spectrum revealed. Owen et al. (1993) discovered

N_2 and CO in the spectrum of Pluto using the same instrument that revealed CO and CO_2 on Triton, showing a wealth of detail in the CH_4 bands as well (Figure 1). Nitrogen vapor over the N_2 ice at a plausible surface temperature was thus identified as the bulk atmospheric constituent. Although the surface pressure of the N_2-dominated atmosphere is not known, it probably exceeds 50 microbars, and it contains about 1 % CH_4 (Young 1994).

Atmospheric aerosols and hazes analogous to those seen by Voyager on Triton are expected on Pluto, but there is no information on the possibility of active plumes transferring material from the surface (or subsurface) to the atmosphere, as seen on Triton. Pluto's atmosphere is certainly transparent, as evidenced by the large amplitude and repeatability of the rotational lightcurve.

The albedo of Pluto increases toward longer wavelengths in the region 0.3-0.8 μm as measured in 1979, but the slope is less than that of Triton measured in the same year. Ultraviolet spectra of Pluto from the Hubble Space Telescope have not yet been published.

We continue by describing the surface components of Pluto in the same way as those of Triton were presented above. Note that most of the spectroscopic and photometric observations of Pluto obtained from ground-based telescopes are measurements of Pluto and Charon together, because the two cannot be readily separated with the spatial resolution afforded by most telescopes and their associated instruments. Separation of the spectral contributions of the two bodies has required special circumstances and techniques, as noted below.

While continued progress in the analysis of Pluto's infrared spectrum requires that the contribution of reflected sunlight from Charon be removed from the spectrum of Pluto + Charon, important new understanding was achieved in the early analysis of a new spectrum of high quality by Owen et al. (1993), as presented below.

3.1.1 Nitrogen

The 2.148 μm band of beta N_2 is seen in weak absorption in the spectrum of Pluto and Charon together. Because sunlight reflected from Pluto dominates the signal from Pluto + Charon, the N_2 absorption is attributed to Pluto. The N_2 band has the

same basic characteristics as it does in Triton's spectrum; the temperature sensitivity of the profile and substructure in the band have been used to derive a temperature of 40 (+/- 2) K for the N_2-covered regions of Pluto from data of May 1993 when the planet was 29.74 AU from the Sun (Tryka et al. 1994). The condensation and sublimation is expected to maintain an isothermal N_2 distribution, although this temperature should vary with the planet's changing heliocentric distance. Whether the temperature of N_2 can fall below the α-β phase transition temperature into the α region is not known. Stansberry et al. (1995) consider the change in infrared emissivity of the two phases and conclude that the temperature should remain in the beta region throughout Pluto's year.

Quirico and Schmitt (1995) showed that the frequency of the CH_4 bands favor a surface temperature close to the α-β transition temperature of 35.6 K (see below), and, for the same reasons as for Triton, Quirico et al. (1995) argue that the presence of α N_2 on Pluto cannot yet be excluded.

Even though the N_2 band on Pluto is somewhat weaker than that on Triton, this ice must cover a significant fraction of the planet's surface (though not all). The mean pathlength through solid N_2 that a photon must traverse in order to produce the observed absorption is several cm.

3.1.2 Methane

A large number of CH_4 bands are seen in Pluto's spectrum These bands are characteristically stronger than the same bands seen on Triton (Owen et al. 1993), and the scattering models of synthetic spectra calculated in a similar way to those for Triton show a significantly larger mass fraction of CH_4 to N_2.

As with Triton, the CH_4 bands on Pluto are seen to be shifted to shorter wavelengths than the bands have in spectra of pure CH_4. This indicates that at least some of the CH_4 on Pluto is dissolved in the matrix of N_2. From the analysis of the positions of the CH_4 bands with the laboratory data on CH_4 diluted in N_2 (see Triton section above), Quirico and Schmitt (1995) suggest that CH_4 is diluted in α and/or possible β N_2 close to, or at the α-β transition temperature (35.6 K), in agreement with the lowest values found for the surface temperature of Pluto, but possibly in disagreement with the

teemperature (40 ± 2 K) derived from the N_2 band by Tryka et al. (1994).

The spectra of Pluto analyzed and published by Owen et al. (1993) were obtained at spectral resolution 350, which is sufficient to show the CH_4 band shift. Subsequent spectra obtained a twice that resolution appear to show a doubling of the CH_4 bands, indicating two reservoirs of this molecule on Pluto's surface, one in which CH_4 is dissolved in the N_2 and one that may be freely exposed on the surface. In their investigation of the hypothesis of large amounts of CH_4 on Pluto, Quirico et al. (1995) presented their first results of a systematic study of CH_4:N_2 mixtures with high fractional abundances of CH_4. From a spectroscopic analysis of the bands, Schmitt et al. (1994) favor a vertical segregation of CH_4 with an enriched top layer, rather than a horizontal distribution of patches of pure and diluted CH_4. The details of the geometric relationship of these two reservoirs is presently under investigation by B. Schmitt and his colleagues.

The best fitting molecular mixture models calculated by Owen et al. (1993) have 1.5% CH_4 relative to N_2, with an uncertainty in this amount of a factor of 2 to 4. Owen et al. acknowledged the shortcomings of their models, noting that adequate optical constants for true molecular mixtures of CH_4:N_2 were not available.

3.1.3 Carbon Monoxide

The (2-0) band of CO at 2.35 μm is seen in Pluto's spectrum, though it is weaker than on Triton. For the same reasons as discussed for Triton, the CO is expected to be dissolved in the N_2, but the matrix wavelength shift is too small to be detected in the present data. The molecular mixture models of Owen et al. (1993) yielded a best fit for 0.5% CO with grain size 0.5 mm, also with a factor of 2 to 4 uncertainty.

3.1.4 Other Volatile Components

While CO_2 is clearly present on Triton, there is no spectral evidence for it on Pluto, even in higher resolution data taken since the original work by Owen et al. (1993). The spectrum was also scrutinized for signatures of other hydrocarbons and nitriles, as well as H_2O. Because the spectral signature of H_2O

is broad, even the signature of the H_2O on Charon (see next section) mixed with the spectral signal of Pluto is not readily evident in the data.

Owen et al. (1993) found no evidence in Pluto's spectrum for C_2H_2, C_2H_4, C_2H_6, H_2O, H_2S, CH_3OH, or NH_3. Independent laboratory studies of possible minor amounts of various hydrocarbons in Pluto's N_2 matrix by Schmitt and Quirico (1992), Bohn et al. (1994), and Quirico and Schmitt (1995) revealed no new identification, although Bohn et al. noted that a mixture of branched alkanes in the N_2 matrix might account for discrepancies between the Owen et al. model and Pluto's spectrum.

The situation with neon and argon on Pluto is similar to that described above for Triton. Neither atom is detectable in the spectral region covered by the near-infrared data, but independent information on the atmosphere of Pluto derived from the stellar occultation in 1988 shows that the mean molecular weight of the atmosphere is consistent with a composition that is 99% N_2. If Ne or Ar occurred on Pluto's surface, their high volatility would ensure a major contribution to the atmosphere. The bulk density of Pluto is strongly indicative of the presence of a major fraction of H_2O ice in its interior. The apparent lack of Ne in Pluto's atmosphere suggests that the ices in the interior of Pluto accreted at temperatures above 20K (Laufer et al. 1987, Owen et al. 1993).

3.1.5 Non-volatile Components of Pluto's Surface

Pluto's surface is not entirely covered by N_2 ice and its incorporated molecular material. Large regions, particularly near the equator, have a significantly lower albedo than expected for a predominantly icy surface. The temperature of these lower albedo regions is too high to be consistent with solid N_2 (Tryka et al. 1994), although H_2O ice contaminated with low-albedo particulate material might occur there and remain stable over the age of Pluto. In any event, the composition of the dark material is of special interest because of the possibility that it consists of carbon or carbon-rich molecular solids. Photochemical products from ultraviolet irradiation of Pluto's N_2/CH_4 (with possible CO) atmosphere, or organics produced by irradiation of the surface ices may constitute or contribute to this dark matter. There is presently no spectral evidence that bears directly upon this question.

3.1.6 Pluto Summary

Pluto's variegated surface is covered in part by large expanses of solid N_2 with CH_4 and CO incorporated as a solid solution. Some expanses of pure CH_4 may also exist, but the geometry of the layers and areas covered by various pure and mixed volatiles has not yet been elucidated through the analysis of the spectral data. That portion of the surface that is covered by volatiles, whatever their mixing and layering relationships, regulates the surface pressure and composition of the atmosphere. Variations in the volatile temperature and the consequent changes in the atmospheric pressure and structure over Pluto's seasonal cycle are subjects of considerable current interest and study, but are outside the scope of this chapter.

3.2. Charon

The total eclipses of Charon by Pluto that occurred during the epoch of mutual transits and eclipses in the 1980s afforded opportunities to determine the spectral reflectance of Charon without the interference of light from Pluto itself (Buie et al. 1987, Marcialis et al. 1987, Fink and DiSanti 1987). Fink and DiSanti (1987) found no spectral features attributed to Charon in the region 0.6-1.0 μm, and showed that the overall reflectance is neutral in color. In the region 1.5-2.5 μm, Buie et al. (1987) and Marcialis et al. (1987) found absorption bands of H_2O ice on the satellite. The low-resolution spectrum of Charon by Buie et al. (1987) shows H_2O ice bands similar in strength to those on Ganymede, corresponding to a grain size of about 65 μm. Roush (1994) showed that other volatiles in significant quantities are not excluded by the Buie et al. spectrum of Charon; in particular significant amounts of CO_2 and CH_4 are possible under certain plausible conditions of grain size and mixing. Although Roush (1994) did not include other ices in his study, by implication a number of other constituents could exist on Charon in geochemically significant quantities and have escaped detection.

The spectral geometric albedo of Charon is important to establish both for the purpose of modelling Charon itself, and for the process of deriving the spectral geometric albedo of Pluto, since in the observed spectrum the light from both objects is mixed according to their relative dimensions and overall reflectances. Roush et al. (1994, 1996) used the Buie et al. (1987) Charon data

and calculated the geometric albedos of both the planet and the satellite at four wavelengths between 1.5 and 2.35 μm. Combining the geometric albedo results for Charon from the Buie et al. (1987) and the Fink and DiSanti (1987) segments of the spectrum, Roush et al. (1994, 1996) found that an intimate mixture of 88% H_2O ice with grain size 65 μm and 12% graphite with grain size 50 μm provides a satisfactory fit to both the H_2O band depths and the geometric albedo between 0.6 and 2.44 μm (Figure 2). Graphite is not proposed as the dark component of Charon; it is a convenient material for which the optical constants are known.

Marcialis et al. (1992) used a technique similar to that of Roush et al. (1994, 1996) for calculating the spectral geometric albedo of Charon, but substituting the near-infrared data of Marcialis et al. (1987) for those of Buie et al. (1987). The result was a somewhat different range of values from those of Roush et al.

3.2.1 Charon Summary

The surface of Charon is somewhat darker than that of Pluto, and carries the spectral signature of H_2O ice. There are differing results on the global homogeneity of Charon's surface derived from photometry at several wavelengths (see Cruikshank et al. 1996 for a discussion of these diverse results). Other ices may also exist. The overall low albedo and neutral color outside the H_2O ice bands shows that some gray component of unknown composition is mixed with the ice in some way.

4. General Summary

Triton, Pluto, and Charon are small bodies composed of ices representing the simplest combinations of the cosmically abundant volatile atoms C, H, O, and N. Pluto and Triton are presently the only Solar System bodies known to carry condensed N_2. The compositional relationship of these objects to the large population of Kuiper belt planetesimals (Jewitt and Luu 1995, Weissman 1996, Cruikshank 1996) and to the comets is not yet clear.

5. Appendix: Modeling Reflectance Spectra

5.1 Types of Mixtures

To model the reflectance spectrum the mixing nature of the

various surface components must be considered. Here molecular, intimate, and spatial mixtures are considered in order to include potential mixing of components at a variety of scales. Molecular mixtures describe mixing that occurs while the individual components (e.g. N_2, CH_4, etc.) are gases and then subsequently condensed. The resultant solid is a material with mixing occurring at molecular dimensions. Depending upon the relative abundance and compositions of the components, this mechanism can result in solid solutions, where one component substitutes within the crystal structure of the other, or alternatively matrix isolation, where one component occurs as an isolated molecule trapped in the structural matrix of the other component(s). Intimate mixtures describe the situation where discrete grains of pure materials have condensed separately but the resulting solids have been subsequently mixed together at the micrometer or granular scale. Terrestrial soils or the lunar regolith are examples of intimate mixtures. Spatial mixtures describe mixing of pure materials at macroscopic scales, such as individual outcrops or regions of pure materials.

5.2 Mathematical Modeling

5.2.1 Molecular Mixtures

Mathematical models for calculating the reflectance spectra of surfaces composed of molecular mixtures from the optical properties of the individual components do not exist. The optical properties of the individual components only serve as a guide for where features may be anticipated. However, matrix isolation can result in significant shifts in both the positions and intensities of absorption features (e.g. Van Thiel et al. 1957, Allamandolla 1984, Schmitt et al. 1993). For modeling purposes, the optical properties must be determined from the molecular mixtures and then used to calculate the reflectance for either an intimate or spatial mixture that contains the molecular mixture as one or more components.

5.2.2 Intimate Mixtures - Equations and Assumptions

Hapke (1981, 1984, 1986, 1993a,b) has developed a series of equations, based on a two-stream approximation to the equations of radiative transfer, that provide the ability to calculate the reflectance of intimate mixtures, given assumptions or knowledge of the physical nature and solid phases comprising the surface.

The bidirectional reflectance of a surface, at each wavelength (λ), can be expressed as

$$r(i,e,g,\bar{w},h,S(0),b,c,\bar{\Theta}) = \frac{\bar{w}}{4\pi}\frac{\mu_o}{\mu_o+\mu}\{[1 + B(g)]P(g) + H(\mu_o)H(\mu) - 1\}, \quad (1)$$

where i is the angle of the incident light (μ_o = cos i), e is the angle of the emergent light (μ = cos e), g is the phase angle between i and e, $\bar{w}$ is the average single scattering albedo of thesurface, h characterizes the width of the opposition surge in terms of the microstructure of the surface (porosity, particle size distribution, and compaction rate with depth), S(0) is the opposition surge amplitude and characterizes the contribution of light scattered from near the front surface of individual particles at zero phase, b and c are coefficients in the Legendre polynomial model of the average particle phase function, and $\bar{\Theta}$ is the average topographic slope angle of surface roughness at sub-spatial resolution scale. The opposition surge is expressed as

$$B(g) = \frac{B_o}{1 + \frac{\tan\left(\frac{g}{2}\right)}{h}}, \quad (2)$$

where

$$B_o = \frac{S(0)}{\bar{w}P(g=0)} \quad (3)$$

in which S(0) is the fraction of light scattered from close to the surface at g = 0. In all the models we assume h = 0.05 (a lunar-like surface) and S(0) = 1.0. Following the development of Hapke (1981), the phase function is expressed as a Legendre polynomial

$$P(g) = 1 + b\cos(g) + c(1.5\cos^2(g) - 0.5), \quad (4)$$

and in all of the models we assume an isotropic phase function, implying b = c = 0. $H(\mu_o)$ and $H(\mu)$ are Chandrasekhar's H-functions (1960). From equation 17 of Hapke (1981) the average single scattering albedo is

$$\bar{w} = \frac{\sum_{i=1}^{i=n}\frac{M_i}{\rho_i D_i}Q_{Si}}{\sum_{i=1}^{i=n}\frac{M_i}{\rho_i D_i}}, \quad (5)$$

where M_i, ρ_i, and D_i are the mass fraction, solid density, and diameter of the i^{th} particle, respectively. The scattering efficiency of the i^{th} particle (Q_{Si}) is given by equation 24 of Hapke (1981) as

$$Q_S = S_E + \frac{(1-S_E)(1-S_I)\left\{r_1 + e^{-2\frac{D}{3}(\alpha(\alpha+s))^{\frac{1}{2}}}\right\}}{1 - r_1 S_I + (r_1 - S_I)e^{-2\frac{D}{3}(\alpha(\alpha+s))^{\frac{1}{2}}}}, \tag{6}$$

where S_E and S_I are the external and internal, reflection coefficients, r_1 is the bihemispherical reflectance of a semi-infinite medium, α is the volume absorption coefficient inside the particle, and s is the volume scattering coefficient inside the particle (Hapke 1981). S_E is expressed as

$$S_E = \frac{1}{2}(|R_{||}|^2 + |R_{\perp}|^2), \tag{7}$$

where $R_{||}$ and $R_{\perp}$ are the Fresnel reflection coefficients polarized parallel and perpendicular to the incident energy, respectively. Following Hansen and Travis (1974), but replacing their $\sin\gamma$ and $\cos\gamma$ with $\cos(g/2)$ and $\sin(g/2)$, respectively, the Fresnel coefficients are expressed as

$$|R_{\perp}|^2 = \frac{(\cos(\frac{g}{2}) - u)^2 + v^2}{(\cos(\frac{g}{2}) + u)^2 + v^2} \tag{8}$$

and

$$|R_{||}|^2 = \frac{[(n^2-k^2)\cos(\frac{g}{2}) - u]^2 + (2nk\cos(\frac{g}{2}) - v)^2}{[(n^2-k^2)\cos(\frac{g}{2}) + u]^2 + (2nk\cos(\frac{g}{2}) + v)^2}, \tag{9}$$

where

$$u = \left\{\frac{n^2 - k^2 - \sin^2(\frac{g}{2}) + [(n^2 - k^2 - \sin^2(\frac{g}{2}))^2 + 4n^2k^2]^{\frac{1}{2}}}{2}\right\}^{\frac{1}{2}} \tag{10}$$

and

$$v = \left\{\frac{-(n^2 - k^2 - \sin^2(\frac{g}{2})) + [(n^2 - k^2 - \sin^2(\frac{g}{2}))^2 + 4n^2k^2]^{\frac{1}{2}}}{2}\right\}^{\frac{1}{2}}, \tag{11}$$

where n and k are the real and imaginary parts of the complex index of refraction. S_I is equivalent to S_E, but g is integrated over all angles. Hapke (1981) defines r_1 as

$$r_1 = \frac{1 - \left(\frac{\alpha}{\alpha + s}\right)^{\frac{1}{2}}}{1 + \left(\frac{\alpha}{\alpha + s}\right)^{\frac{1}{2}}} . \qquad (12)$$

The volume absorption coefficient, α, is related to the imaginary index of refraction through the dispersion relation

$$\alpha = \frac{4\pi k}{\lambda} , \qquad (13)$$

and in all the models we assume minimal internal scattering, and hence let $s = 10^{-17}$. Hapke (1984) discussed the influence of macroscopic surface roughness on reflectance and introduced $\bar{\theta}$ to represent the average topographic slope angle of surface roughness. This effect is not included in the calculations presented here.

5.3 Spatial Mixtures

For spatial mixtures, the reflectance of the individual components are calculated using equations 1-13 above. These reflectances are then combined at each wavelength to represent the total reflectance (R_T) of a spatial mixture via:

$$R_T = (A * R_A) + (B * R_B) + \cdots (N * R_N) \qquad (14)$$

where R_A, R_B, and R_N are the reflectances and A, B, and N represent the areal extent or spatial coverage of each component such that they sum to 1.0, respectively.

5.3.1 Optical Constants

5.3.1.1 Molecular Mixtures

The real and imaginary indices of refraction of molecular mixtures must be determined on a mixture-by-mixture basis. While these values are available in the mid- and far-infrared for a variety of mixtures (e.g., Hudgins et al. 1993), their

availability in the near-infrared is extremely limited (Sill et al. 1980; Pearl et al. 1991; B. Schmitt, personal communication 1992; D. Hudgins, personal communication 1991). As a result, we have not modeled such mixtures, even though it appears that CH_4 is dissolved in N_2 on both Pluto (Owen et al. 1993) and Triton (Cruikshank et al. 1993). For the calculations here we have simulated the positions of the absorption bands produced in molecular mixtures by shifting the peak values of the imaginary index of refraction of pure CH_4 to the corresponding amount of the shift present in the observational data.

5.3.1.2 Intimate and Spatial Mixtures

The real and imaginary indices of refraction of the various ices used in these calculations (equations 6-13) are from a variety of sources. Values for H_2O ice are taken from Warren (1984), the values for both CO and CH_4 ice were provided by Bernard Schmitt (Schmitt et al. 1992), and the values for β-N_2 were provided by Robert Brown (Green et al. 1991). These refractive indices were convolved to the same resolution as the observational data using a Gaussian to represent the bandpass of the telescopic instrument.

5.4 Caveats

As outlined in the equations above, the calculated reflectances are directly influenced by any changes in the optical constants used in a calculation. If the optical constants are revised or supplanted by newer more accurate values, then the results and conclusions presented here should be reviewed. Additionally, if the optical constants were determined from ices at a significantly different temperature than Pluto (≈30-45K) and there is a strong dependance of the optical constants on temperature, then the discussions and conclusions below may be influenced.

5.5 Improving the Models

As more observational data become available, at these and other wavelengths, it is imperative to the modeling effort that appropriate and accurate optical constants are available. For example, recent laboratory measurements by Grundy et al. (1993a,b) and Schmitt et al. (1992) are providing information for CH_4 in the 0.68-2.5 μm region that will be useful in modeling

historic (Grundy and Fink 1993) and continuing observations of Pluto. Schmitt et al. (1993) are investigating the effects of temperature, concentration of CH_4, and crystallization history on the optical properties of N_2:CH_4 molecular mixtures that will be useful in future modeling. Consideration of anisotropic scattering may provide a means of reducing some of the remaining discrepancy between the models and observational data. However, care must be taken to ensure that data collected at all wavelengths are directly comparable and do not sample different portions of the rotational phase curve. Even then, retaining absolute albedo information requires more specific knowledge regarding the relative contribution of Charon. Ideally, separate spectra of Pluto and Charon should be obtained simultaneously over the entire wavelength region of interest.

6. Acknowledgments

This research is supported by NASA Planetary Astronomy RTOP 196-41-67-03 (Cruikshank), NASA Planetary Geology and Geophysics RTOP 151-01-60-01 (Roush), and a grant from the NASA Planetary Astronomy program (Owen).

7. References

Allamandola, L. J. (1984) Absorption and Emission Characteristics of Interstellar Dust. In Kessler, M. F. and Phillips, J. P. (eds.) Galactic and Extragalactic Infrared Spectroscopy, Reidel, Dordrecht, 5-35.

Bohn, R. B., Sandford, S. A., Allamandola, L. J. and Cruikshank, D. P. (1994) Infrared spectroscopy of Triton and Pluto ice analogs: The case for saturated hydrocarbons, Icarus, 111, 151-173.

Broadfoot, A. L. and the Voyager UVS Team (1989) Ultraviolet spectrometer observations of Neptune and Triton, Science, 246, 1459-1466.

Brown, G. N., Jr. and Ziegler, W. T. (1979) Vapor pressure and heats of vaporization and sublimation of liquids and solids of interest in cryogenics below 1-atm pressure. In Timmerhaus, K. D. and Snyder, H. A. (eds.) Advances in Cryogenic Engineering, Vol. 25, Plenum Press, New York, pp. 662-670.

Brown, R. H., Cruikshank, D. P., Veverka, J., Helfenstein, P. and Eluszkiewicz, J. (1995) Surface composition and photometric properties of Triton. In Cruikshank, D. P. (ed.) Neptune and Triton. Univ. of Arizona Press, Tucson, pp ***-***.

Buie, M. W. (1984) Lightcurve CCD Spectrophotometry of Pluto, Ph.D. dissertation, Univ. of Arizona, 102 pp.

Buie, M. W. and Fink, U. (1987) Methane absorption variations in the spectrum of Pluto, Icarus, 70, 483-498.

Buie, M. W., Cruikshank, D. P., Lebofsky, L. A. and Tedesco, E. F. (1987) Water frost on Charon, Nature, 329, 522-523.

Chandrasekhar, S. (1960) Radiative Transfer, Dover, New York, 393pp.

Christy, J. W. and Harrington, R. S. (1978) The satellite of Pluto, AJ, 83, 1005-1008.

Cruikshank, D. P., Pilcher, C. B. and Morrison, D. (1976) Pluto:

Evidence for methane ice, Science, 194, 835-387.

Cruikshank, D. P. and Apt, J. (1984) Methane on Triton: Physical state and distribution, Icarus, 58, 306-311.

Cruikshank, D. P., Brown, R. H. and Clark, R. N. (1984) Nitrogen on Triton, Icarus, 58, 293-305.

Cruikshank, D. P. and Silvaggio, P. M. (1979) Triton: A satellite with an atmosphere, ApJ, 233, 1016-1020.

Cruikshank, D. P. and Silvaggio, P. M. (1980) The surface and atmosphere of Pluto, Icarus, 41, 96-102.

Cruikshank, D. P. (1996) Organic solids in the outer solar system: Kuiper belt planetesimals. In Greenberg, J. M. (ed.) conference volume from the International School of Space Chemistry, Erice, Italy, June 1994 (in press).

Cruikshank, D. P., Roush, T. L., Owen, T. C., Geballe, T. R., de Bergh, C., Schmitt, B., Brown, R. H. and Bartholomew, M. J. (1993) Ices on the surface of Triton, Science, 261, 742-745.

Cruikshank, D. P., Roush, T. L., Moore, J., Sykes, M., Owen, T. C., Brown, R. H. and Tryka, K. A. (1996). The surfaces of Pluto and Charon. In Stern, S. A. and Tholen, D. J. (eds.) Univ. of Arizona Press, Tucson (in press).

Duxbury, N. S. and Brown, R. H. (1993) The phase composition of Triton's permanent polar caps, Science, 261, 748-751.

Elliot, J. E., Dunham, E. W., Bosh, A. S., Slivan, S. M., Young, L. A., Wasserman, L. H. and Millis, R. L. (1989) Pluto's atmosphere, Icarus, 77, 148-170.

Fink, U. and DiSanti, M. A. (1987) The separate spectra of Pluto and its satellite Charon, AJ, 95, 229-236.

Green, J. R., Brown, R. H., Cruikshank, D. P. and Anicich, V. (1991) The absorption coefficient of nitrogen with application to Triton, Bull. Amer. Astron. Soc., 23, 1208 (abstract).

Grundy, W. M. and Fink, U. (1993) CCD spectra of Pluto from 1982 to present, Bull. Am. Astron. Soc., 25, 1131 (abstract).

Grundy, W. M., Schmitt, B. and Quirico E. (1993a) Temperature dependent absorption spectra of CH_4 and N_2 ices, Bull. Am. Astron. Soc., 25, 1132 (abstract).

Grundy, W. M., Schmitt, B. and Quirico, E. (1993b) The temperature dependent spectra of alpha and beta nitrogen ice with application to Triton, Icarus, 105, 254-258.

Hansen, J. E. and Travis L. D. (1974) Light scattering in planetary atmospheres, Space Sci. Rev., 16, 527-610.

Hapke, B. W. (1981) Bidirectional reflectance spectroscopy I. Theory, J. Geophys. Res., 86, 3039-3054.

Hapke, B. W. (1984) Bidirectional reflectance spectroscopy 3. Correction for macroscopic roughness, Icarus, 59, 41-59.

Hapke, B. W. (1986) Bidirectional reflectance spectroscopy 4. The extinction coefficient and the opposition effect, Icarus, 67, 264-280.

Hapke, B. W. (1993a) Combined theory of reflectance and emittance spectroscopy. In Pieters, C. M. and Englert, P. A. J. (eds.) Remote Geochemical Analysis: Elemental and Mineralogical Composition. Cambridge Univ. Press, New York, pp 31-42.

Hapke, B. W. (1993b). Reflectance and Emittance Spectroscopy. Cambridge Univ. Press, New York, 455 pp.

Herbert, F. and Sandel, B. R. (1991) CH_4 and haze in Triton's lower atmosphere, J. Geophys. Res., 96, 19241-19252.

Hudgins, D. M., Sandford, S. A., Allamandola, L. J. and Tielens A. G. G. M. (1993) Mid- and far-infrared spectroscopy of ices: Optical constants and integrated absorbances, ApJS, 86, 713-870.

Jewitt, D. C. and Luu, J. X. (1995) The solar system beyond Neptune, AJ, 109, 1867-1876.

Laufer, D., Kochavi, E. and Bar-Nun, A. (1987) Structure and dynamics of amorphous water ice, Phys. Rev. B., 36, 9219-9227.

Löwen, H. W., Bier, K. D. and Jodl, H. J. (1990) Vibron-phonon

excitations in the molecular crystals N_2, O_2, and CO by Fourier transform infrared and Raman studies, J. Chem. Phys., 93, 8565-8575.

Lunine, J. I., Atreya, S. K. and Pollack, J. B. (1989) Present state and chemical evolution of the atmospheres of Titan, Triton and Pluto. In Atreya, S. K., Pollack, J. B., and Matthews, M. S. (eds.), Origin and Evolution of Planetary and Satellite Atmospheres, Univ. of Arizona Press, Tucson, 605-665.

Marcialis, R. L., Rieke, G. H. and Lebofsky, L. A. (1987) The surface composition of Charon: Tentative identification of water ice, Science, 237, 1349-1351.

Marcialis, R. L. and Lebofsky, L. A. (1991) CVF spectrophotometry of Pluto: Correlation of composition with albedo, Icarus, 89, 255-263.

Marcialis, R. L., Lebofsky, L. A., DiSanti, M. A., Fink, U., Tedesco, E. F. and Africano, J. (1992) The albedos of Pluto and Charon: Wavelength dependence, AJ, 103, 1389-1394.

McKinnon, W. B., Lunine, J. I. and Banfield, D. (1995) Origin and evolution of Triton. In Cruikshank, D. P. (ed.) Neptune and Triton. Univ. of Arizona Press, Tucson, pp ***-***.

Owen, T. C., Roush, T. L., Cruikshank, D. P., Elliot, J. L., Young, L. A., de Bergh, C., Schmitt, B., Geballe, T. R., Brown, R. H. and Bartholomew, M. J. (1993) Surface ices and the atmospheric composition of Pluto, Science 261, 745-748.

Pearl, J., Ngoh, M, Ospina, M. and Khanna R. (1991) Optical constants of solid methane and ethane from 10,000 to 450 cm_{-1}, J. Geophys. Res., 96, 17,477-17,482.

Quirico, E. and Schmitt, B. (1995). Near infrared spectroscopy of simple hydrocarbons and carbon oxides diluted in solid N_2 and as pure ices: Implications for Triton and Pluto, Icarus (submitted).

Quirico, E., Schmitt, B., Bini, R. and Salvi, P. R. (1995) The spectroscopy of ices: Physical aspects and astrophysical implications, Planet. Space Sci. (submitted).

Roush, T. (1994) Charon: More than water ice? Icarus, 108, 243-254.

Roush, T., Pollack, J. B., Cruikshank, J. B., Young, E. F. and Bartholomew, M. J. (1994) Geometric albedo of Charon, Bull. Amer. Astron. Soc., 26, 1169 (abstract).

Roush, T., Cruikshank, D. P., Pollack, J. B., Young, E. F. and Bartholomew, M. J. (1996) Near-infrared geometric albedos of Charon and Pluto: Constraints on Charon's surface composition, Icarus (in press).

Sagan, C. and Khare, B. N. (1979) Tholins: Organic chemistry of interstellar grains and gas, Nature, 277, 102-107.

Sagan, C. and Thompson, W. R. (1984) Production and condensation of organic gases in the atmosphere of Titan, Icarus, 59, 133-161.

Schmitt, B. and Quirico, E. (1992) Laboratory data on near-infrared spectra of ices of planetary interest, Bull. Amer. Astron. Soc., 24, 968 (abstract).

Schmitt, B., Quirico, E. and Lellouch, E. (1992) Near infrared spectra of potential solids at the surface of Titan, Proc. Symp. Titan, ESA SP-338, 383-388.

Schmitt, B., Quirico, E., de Bergh, C., Owen, T. C. and Cruikshank D. P. (1993) The near-infrared spectra of Triton and Pluto: A laboratory analysis of the methane bands, Bull. Am. Astron. Soc., 25, 1129 (abstract).

Schmitt, B., Doute, S., Quirico, E., Benchkoura, A., de Bergh, C., Owen, T. C. and Cruikshank, D. P. (1994) The state and composition of the surface of Pluto: Laboratory experiments and numerical modeling, Bull. Amer. Astron. Soc., 26, 1170 (abstract).

Sill, G. T., Fink, U. and Ferraro J. R. (1980) Absorption coefficients of solid NH_3 from 50 to 7000 cm^{-1}, J. Opt. Soc. Am., 70, 724-739.

Smith, B. A. and the Voyager ISS Team, (1989), Voyager 2 at Neptune: Imaging science results, Science 246, 1422-1449.

Smith, E. V. P. and Gottlieb, D. M. (1974) Solar flux and its variations, Space Sci. Rev., 16, 771-802.

Spencer, J. R., Buie, M. W. and Bjoraker, G. L. (1990) Solid methane on Triton and Pluto: 3-4 micron spectrophotometry, Icarus, 88, 491-496.

Stansberry, J. et al.

Stern. S. A. (1993). Properties and tentative identification of the strongly UV-absorbing surface constituent on Triton, Icarus, 102, 170-173.

Stone, E. C. and Miner, E. D. (1989) The Voyager 2 encounter with the Neptunian system, Science, 246, 1417-1421.

Soifer, B. T., Neugebauer, G. and Matthews, K. (1980) The 1.5-2.5 μm spectrum of Pluto, AJ, 85, 166-167.

Thompson, W. R. and Sagan, C. (1990) Color and chemistry on Triton, Science, 250, 415-418.

Trafton, L. (1984) Large seasonal variations in Triton's atmosphere, Icarus, 58, 312-324.

Tryka, K. A., Brown, R. H., Anicich, V., Cruikshank, D. P. and Owen, T. C. (1993) Spectroscopic determination of the phase composition and temperature of nitrogen ice on Triton, Science, 261, 751-754.

Tryka, K. A., Brown, R. H., Cruikshank, D. P., Owen, T. C., Geballe, T. R. and DeBergh, C. (1994) Temperature of nitrogen ice on Pluto and its implications for flux measurements, Icarus, 112, 513-527.

Van Thiel, M., Decker, E. D. and Pimental G. C. (1957) Infrared studies of hydrogen bonding of water by the matrix isolation technique, J. Chem. Phys., 27, 486-490.

Warren, S.G. (1984) Optical constants of ice from the ultraviolet to the microwave, Appl. Opt., 23, 1206-1225.

Weissman, P. R. (1996) The Kuiper Belt. Ann. Rev. Astron. Astrophys. (in press).

Young, E. F. and Binzel, R. P. (1994) A new determination of radii and limb parameters for Pluto and Charon from mutual event lightcurves, Icarus, 108, 219-224.

Young, L. A. (1994) Bulk Properties and Atmospheric Structure of Pluto and Charon, Ph.D. dissertation, Massachusetts Inst. of Technology, 124 pp.

Figure Captions

Figure 1. Spectral geometric albedos of Triton and the Pluto+Charon pair determined from spectra obtained in 1992. In determining the albedo values, the measured flux at each wavelength was divided by the flux of the Sun (from Smith and Gottlieb (1974), and then corrected for the heliocentric and geocentric distances. The radii used in the calculation were 1350 km for Triton and 1165 km for Pluto. The spectral geometric albedo shown here for Pluto includes the contribution of reflected light from Charon. Prominent solid state absorptions are identified.

Figure 2. The spectral geometric albedo of Charon, compiled from two sources of data, as shown. The solid line is a synthetic reflectance spectrum from a Hapke scattering model using the two components shown. The radius used for Charon is 620 km.

END

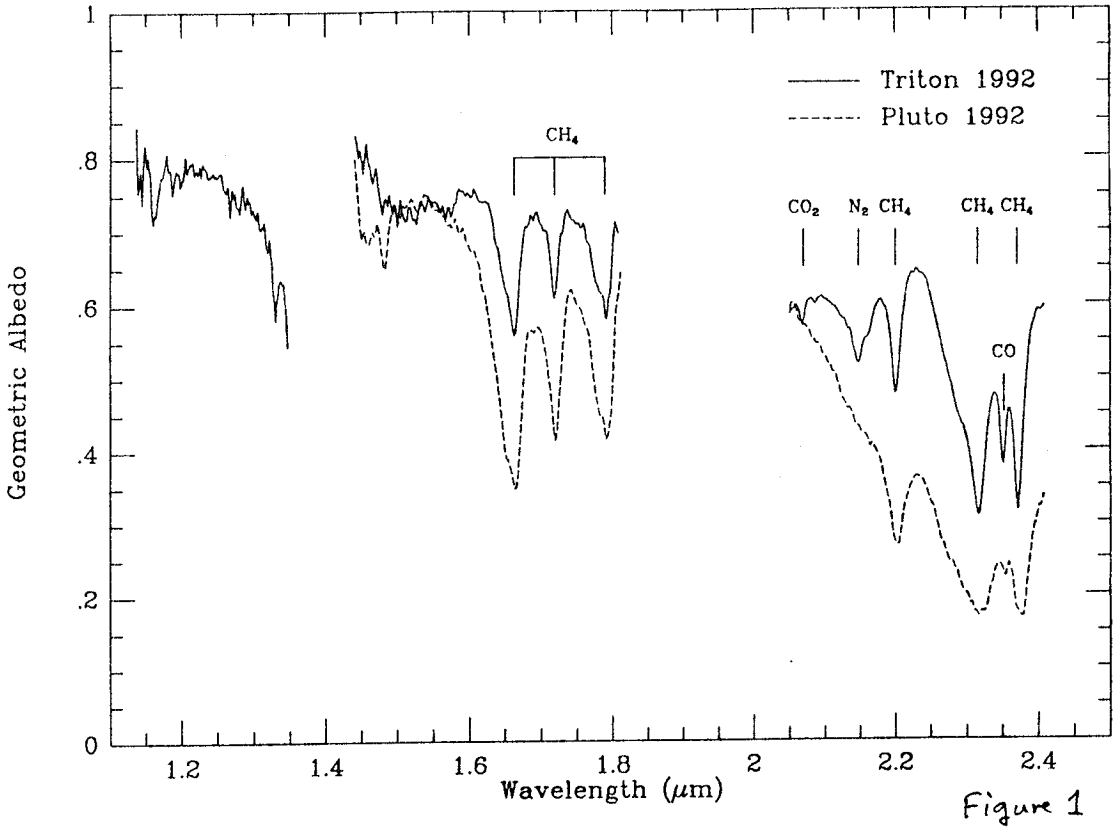

Figure 1

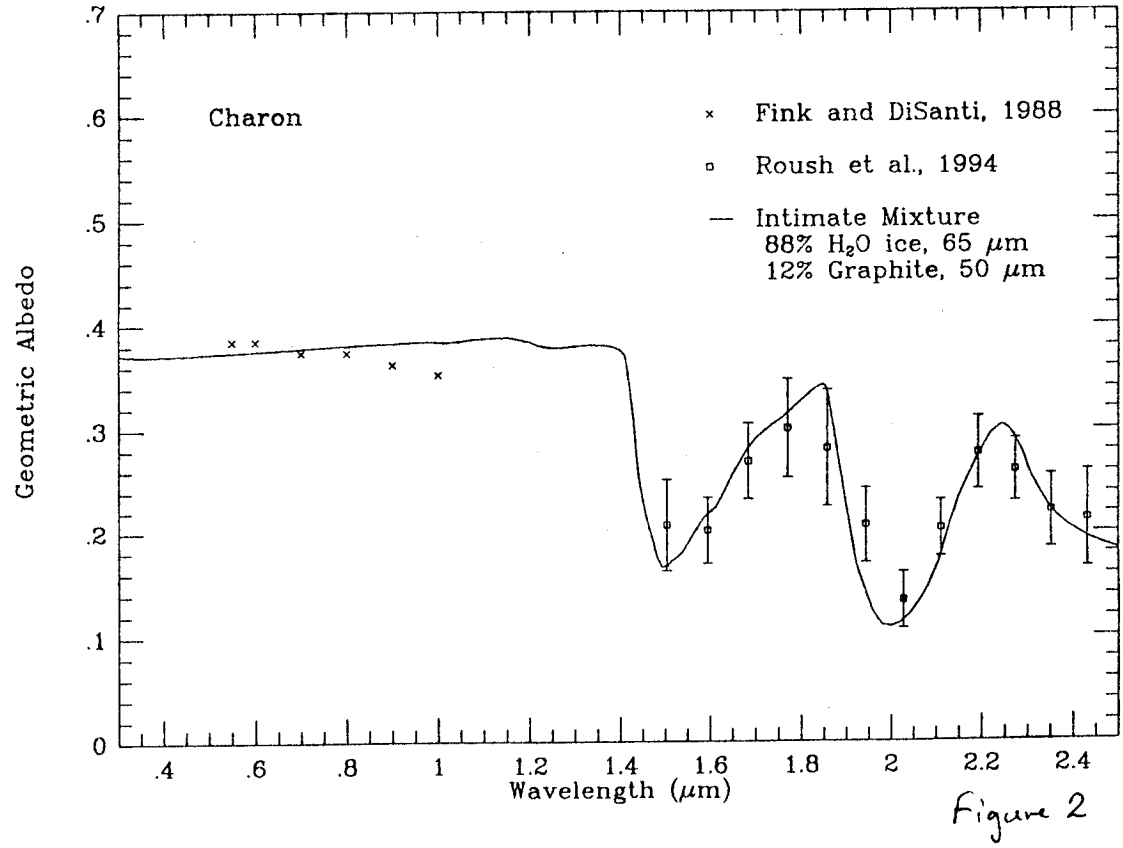

Figure 2